Impact of head models in N170 component source imaging: results in control subjects and ADHD patients

L. Beltrachini[1,†], A. Blenkmann[1,2,†], N. von Ellenrieder[1], A. Petroni[4], H. Urquina[3], F. Manes[3], A. Ibáñez[3,5] and C.H. Muravchik[1]

[1] Laboratory of Industrial Electronics, Control and Instrumentation (LEICI), National University of La Plata.
[2] Epilepsy Center, IBCN - CONICET - University of Buenos Aires.
[3] Institute of Cognitive Neurology (INECO); & Institute of Neuroscience, Favaloro University, Buenos Aires, Argentina.
[4] Integrative Neuroscience Laboratory, Physics Department, University of Buenos Aires, Buenos Aires, Argentina.
[5] Universidad Diego Portales, Santiago, Chile.
[†] Both authors contributed equally to this work

Abstract.
The major goal of evoked related potential studies arise in source localization techniques to identify the loci of neural activity that give rise to a particular voltage distribution measured on the surface of the scalp. In this paper we evaluate the effect of the head model adopted in order to estimate the N170 component source in attention deficit hyperactivity disorder (ADHD) patients and control subjects, considering faces and words stimuli. The standardized low resolution brain electromagnetic tomography algorithm (sLORETA) is used to compare between the three shell spherical head model and a fully realistic model based on the ICBM-152 atlas. We compare their variance on source estimation and analyze the impact on the N170 source localization. Results show that the often used three shell spherical model may lead to erroneous solutions, specially on ADHD patients, so its use is not recommended. Our results also suggest that N170 sources are mainly located in the right occipital fusiform gyrus for faces stimuli and in the left occipital fusiform gyrus for words stimuli, for both control subjects and ADHD patients. We also found a notable decrease on the N170 estimated source amplitude on ADHD patients, resulting in a plausible marker of the disease.

1. Introduction

Researchers use source localization techniques of event-related potential (ERP) to identify the loci of neural activity that give rise to a particular voltage distribution measured on the surface of the scalp. This problem, usually called electroencephalogram (EEG) inverse problem, is affected by the uncertainties of the model used to simulate the situation, such as the head geometry, electrical conductivity or electrode positions. However, it has been shown that if the model used does not differ considerably from the true model, those differences tend to be of the same order of the electronic noise, and then can be individually negligible [1, 2, 3]. To build those realistic models it is necessary to have extra information, usually provided by magnetic resonance images (MRI) and an electrode acquisition system. However, most of ERP studies consist of

making repeated measurements over a large number of patients/controls, making individual model acquisition impractical. Therefore, a standard head model is customarily used.

The simplest and historically accepted model is the three layered homogeneous spherical model, where each layer represents the brain, skull and scalp (inside out), and the electrical conductivities are assumed to be homogeneous and isotropic [4]. As is known, this model has plenty inaccuracies that might affect the EEG forward and inverse problems, such as the lack in geometrical adherence of the assumed shape with respect to a real human head, as well as its simplified electrical conductivity model. In order to avoid these problems, realistic average atlas-based head models jump on stage. These models are generally made from an average of one hundred or more healthy subjects and guarantee an improvement over wrong shaped approximation models [5, 6].

To evaluate the effect of head model on source localization we consider the widely accepted standardized low resolution brain electromagnetic tomography (sLORETA) algorithm [7]. This method allows to localize distributed brain sources by performing a location-wise inverse weighting of the results of a minimum norm least squares analysis with their estimated variances, leading to a smooth solution. Based on the sLORETA we evaluate the impact of the head model in the inverse problem solution by comparing the estimated source variance. We show differences between head models and compute solutions for control subjects and patients.

In this work we focus on solving the EEG inverse problem for the ERP N170 component. The N170 is a cortical marker linked to facial, object and word processing [8, 9]. Several studies have looked for the N170 cortical sources, leading to different solutions. Some of them [9, 10] conclude that the brain generators of this ERP are localized in the fusiform gyri (FG), or in the FG and additional structures such as the lingual gyri [11]. Other works found the brain generators of the same component in the lateral occipital-temporal cortex [12] or in the superior temporal sulci [13]. Those differences may be due to the kind of the stimuli used or to the model assumed to solve the problem. As is shown in this work, unrealistic head models lead to an increase in the localization variance, and therefore its usage cannot be recommended.

We distinguish between control subjects and patients with attention deficit hyperactivity disorder (ADHD). ADHD is a neuropsychiatric condition with onset in childhood that extends over adolescent and adult life with a considerable symptomatic burden and functional impairment. It has been shown [14, 15] that the N170 component represents an ideal brain marker to assess possible cortical markers of emotion processing for faces in ADHD. Therefore, accurate source imaging is fundamental in order to report differences in cortical activation areas between control subjects and ADHD patients. In this work we analyze such differences and show that the spherical head model may lead to erroneous results, even worst if a single dipole model is assumed.

2. Material and Methods

This study is part of a broader research project on the association between cortical processing of facial emotional expressions, social cognition skills and executive functioning [16]. Only relevant data is presented in this work.

2.1. Participants

Ten adult participants with ADHD (one male; three left-handed; mean age of 33.1 years old, standard deviation of 3.42 years old) and ten healthy subjects (one male; two left handed; mean age of 33.3 years old, standard deviation of 3.64 years old) were recruited. ADHD was diagnosed according to the American Psychiatric Association criteria [17], and a questionnaire was given to healthy participants to rule out hearing, visual, psychiatric or neurological deficits. All participants gave signed, informed consent in agreement with the Helsinki declaration. All

experimental procedures were approved by the Ethics Committee of the Institute of Cognitive Neurology. More details regarding participants selection procedure may be found in [16].

2.2. ERP stimuli

Faces and word images were presented to test the effects of stimulus type (faces, words or face-word stimuli), valence (positive vs. negative) and compatibility (compatible vs. incompatible in word and face valence combinations) in a dual valence task. Participants were asked to categorize words or faces displayed on a computer screen according to their valence, into one of two categories (positive or negative), as quickly as possible. In this study variations due to valence and compatibility were not analyzed, i.e. only the three different stimuli type were studied: faces, words and combined face-word. The task comprised of two blocks of 320 trials each, the simultaneous stimuli and the single stimuli block.

Figure 1 shows a diagram of the experimental design. Trials started with a fixation cross for 1000 ms. Then a stimulus was presented for 100 ms, followed by a fixation cross until participants responded. If the response was incorrect, a red cross was presented as feedback for 100 ms and the trial ended. No feedback was provided in trials with correct responses. After responses or feedback, an inter-stimulus interval (ISI) of 1000 ms was added.

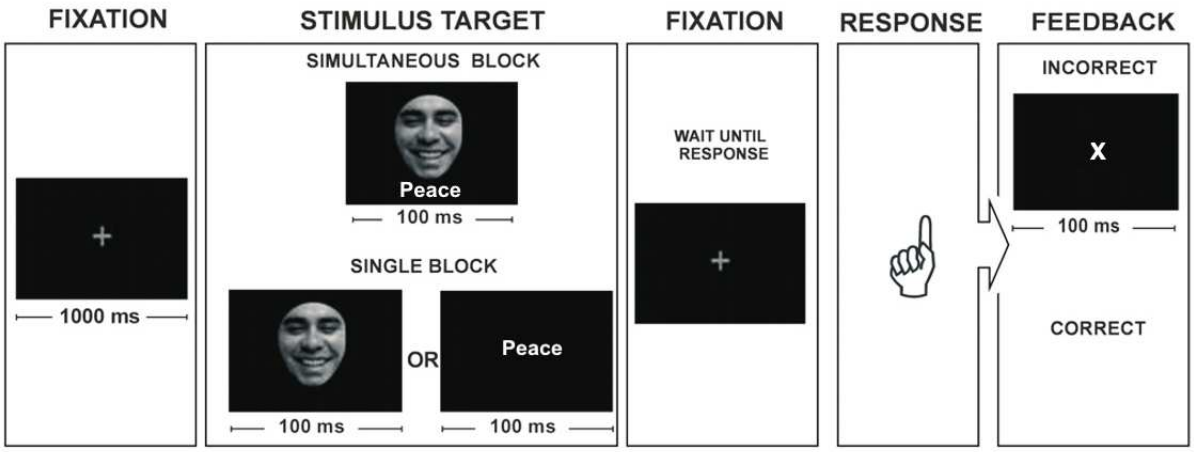

Figure 1. Experimental design. The trial started with a fixation cross, followed by a target stimulus (face or word) or two simultaneous stimuli (face and word) depending on which of the two main blocks was being performed. After the target stimulus, a fixation cross appeared until the response. If the response was incorrect, a red cross appeared and the trial ended. Otherwise, the trial ended without feedback. After responses or feedback, an ISI of 1000 ms was added (not shown).

In the simultaneous stimuli block, participants were exposed in each trial to a face in the center of the screen and a word four degrees below, simultaneously for 100 ms. Participants were asked to indicate the emotion shown by the face and to ignore the word. In the single stimulus block, participants were exposed on each trial to a face or a word in the center of the screen and asked to indicate the emotion of the stimulus. More details regarding experimental conditions can be found in [16].

2.3. Data acquisition

EEG signals were recorded with a BioSemi 128-channel system (BioSemi, Amsterdam, the Netherlands). Sampling rate was set at 500 Hz and signals were band-pass filtered between

0.1 and 100 Hz. Then, data were filtered off-line to remove unwanted frequency components between 0.3 and 30 Hz, down-sampled to 128 Hz and re-referenced to instantaneous average potential. Two bipolar derivations monitored vertical and horizontal ocular movements. EEG data were segmented from 200 ms prior, to 800 ms after the stimulus onset. All segments with eye movement contamination were removed from further analysis using an automatic algorithm [18] and a visual procedure. Only artifact-free segments were averaged to obtain ERPs.

2.4. Head model and forward problem

In order to solve the inverse problem we must first choose a head model. Since individual MRI data was not available, a standard model was considered. The first model proposed was the widely used three layered isotropic spherical model, where each sphere represents the boundaries of different tissue domains (i.e., brain, skull and scalp). The electrical conductivities adopted for each layer are the accepted 0.33 S/m for the brain and scalp, and 0.0096 S/m for the skull [19].

The second model considered in the present study was an average head model built from a sample of 152 MRIs of typical participants provided by the International Consortium of Brain Mapping (ICBM) [20]. The scalp and skull surfaces were extracted from the image using the brain extraction tool [21] and then corrected using MeshLab. To make a fully realistic model we considered the white matter anisotropy using a diffusion tensor atlas based on 81 healthy participants [22] co-registered with the ICBM model. This allows to consider the electrical conductivity as a tensor field through a linear transformation of the diffusion tensor eigenvalues [23]. In Figure 2(a) we show a sagital slice ($x = 9$ in the Montreal Neurological Institute coordinate system) where the boundary surfaces of both models are overlapped. There can be seen the geometric differences between them. In Figure 2(b) we show in the same slice the electrical conductivity map (mean conductivity across each voxel) considered for the realistic (average) model.

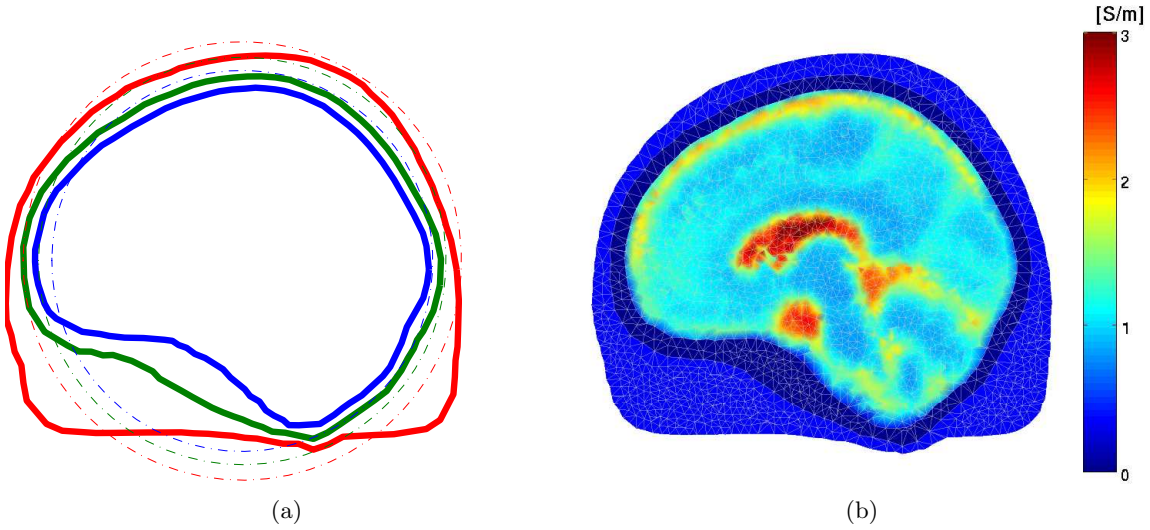

(a) (b)

Figure 2. Head models considered in this work. In Figure 2(a) a sagital slice where both models are overlapped is shown. In Figure 2(b) we show the real-shaped model tessellation colored by the electrical conductivity map (mean conductivity).

In order to solve the EEG forward problem we use the linear finite element method (FEM) [24]. This method, unlike the boundary element method, allows to handle anisotropy of the electrical conductivity in the soft tissues. The original models were tessellated using the ISO2Mesh toolbox [25], resulting a tetrahedral mesh with 2 mm side length average (see

Figure 2(b)). Possible solutions were constrained to the cortical surface but were not constrained for orientation [6].

2.5. Source imaging

To localize the generators of brain activity we considered the widely accepted sLORETA [7]. This is a statistical source imaging method that performs a distributed and smooth source localization. Although its solution is a distributed source activation map, it has been shown that sLORETA method localizes dipolar sources with zero error under ideal conditions [26, 27], allowing its usage also for dipolar source estimation. Therefore, it can be used to compare both dipolar and distributed solutions.

Basically, sLORETA employs a minimum norm current density estimation, and then localization is computed by standardizing the obtained values with respect to the variance of those estimators, leading to the here called source current power density (SCPD) factor. This estimation is done by assuming that the current density variance receives contributions from possible noise in the EEG measurements due to electric neuronal activity. In its simplest form, this noise can be assumed to be independent and identically distributed all over the cortex, allowing equal contribution of all cortical neurons to the biological noise. Under these conditions, it can be shown [7] that the estimated current density covariance matrix $\mathbf{S}_{\hat{\mathbf{j}}}$ depends only on the head model used to compute the forward problem, and then can be used to compare the influence of models in the EEG inverse problem. To quantify this influence we compute the ratio between the mean variance of the estimated current density across the directions for both spherical and realistic head models, i.e.

$$R_l = \frac{tr\left\{\left[\mathbf{S}_{\hat{\mathbf{j}}_S}\right]_l\right\}}{tr\left\{\left[\mathbf{S}_{\hat{\mathbf{j}}_R}\right]_l\right\}}, \tag{1}$$

where $tr\{\cdot\}$ is the trace operator, S and R refers to the spherical and realistic head models, and the l subindex refers to the lth test location over the cortex. Equation (1) allows to compare between the variance of the estimated current density map for both spherical and realistic head models. If the mean value of the estimated current density is of the same order for both models, the variance ratio will account for the differences on the SCDP factor, and then will explain differences on source location. Larger variance ratio values will be associated with cortex regions where the realistic model improves the source localization over the spherical model. We refer to [7] for sLORETA related formulae.

2.6. Data selection

sLORETA images were calculated at N170 component negative peak for each subject and condition using a spherical and a realistic head model. To determine the N170 peak, the average signal of representative electrodes over occipital lobes was obtained (see Figure 3), within a 167-229 ms time window for faces and simultaneous faces-words stimuli, and within a 182-284 ms time window for word stimuli, for each subject. The N170 peak amplitude was found as the local minimum of this average.

SCDP was calculated for each condition and subject using sLORETA method with the presented head models at the N170 peak. Finally, the average of this source images for faces, words and simultaneous faces-words stimuli were obtained for both groups under study (patients and controls).

3. Results

In this Section we show results concerning the N170 component source localization considering both realistic and spherical head models, for control subjects and ADHD patients. First we

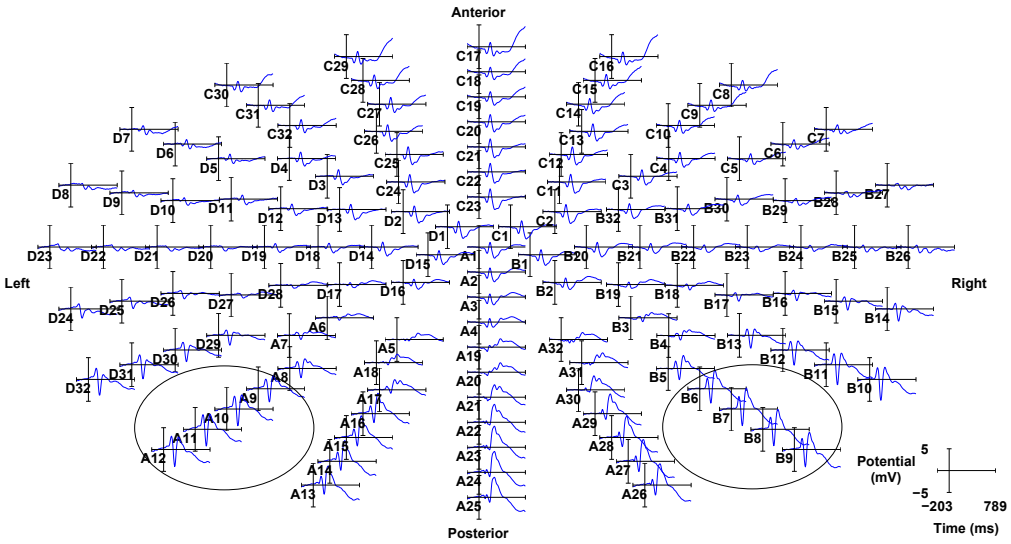

Figure 3. Measured potentials placed in the 128 electrode BioSemi standard position. Representative electrodes are marked (see Section 2.6).

perform the source localization. For each subject and condition two sLORETA source images were obtained at N170 peak, one for each head model. These images were averaged across control subjects (Figure 4) and ADHD patients (Figure 5).

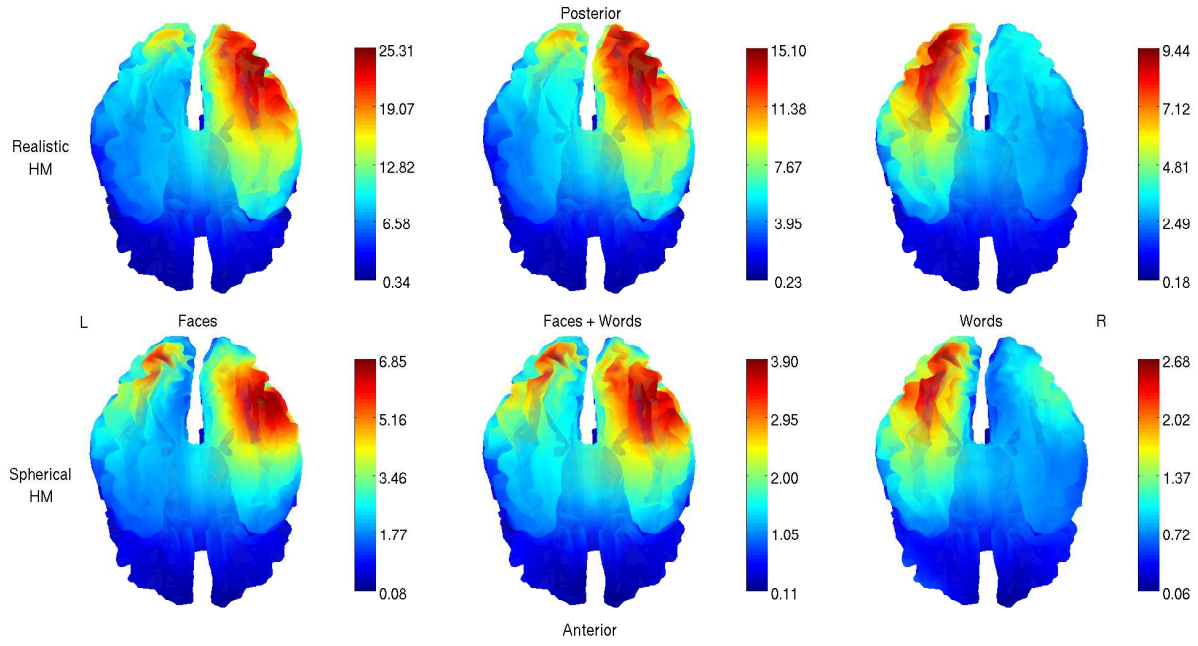

Figure 4. sLORETA source images (SCDP$\times 10^{-6}$) of N170 component peak for control subjects using the realistic head model (upper row) and the spherical head model (lower row) from a basal view. Three different stimuli are depicted: faces (first column), simultaneous faces and words (second column) and words (third column).

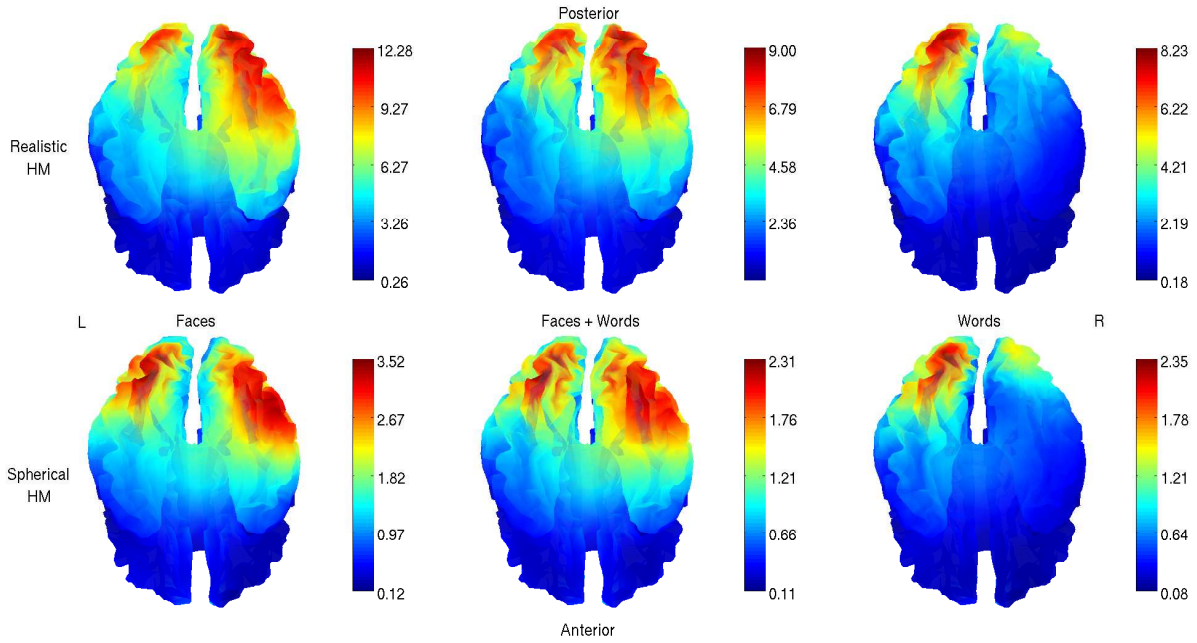

Figure 5. sLORETA source images (SCDP$\times 10^{-6}$) of N170 component peak for ADHD patients using the realistic head model (upper row) and the spherical head model (lower row) from a basal view. Three different stimuli are depicted: faces (first column), simultaneous faces and words (second column) and words (third column).

In a general view, all images obtained using the spherical head model found the activation zones in more anterior areas and more bilateral than using the realistic model. The intensity of SCDP is considerably larger in the realistic model, implying more reliable solutions to the inverse problem. These differences may be decisive if only one dipolar source placed on the test point where the SCDP is maximum is considered. Table 1 shows the different MNI coordinates and the anatomical description obtained from the Harvard-Oxford Cortical Structural Atlas [28] of these maxima. When the realistic head model was used, maximum SCDP values for faces and simultaneous faces-words stimuli in control subjects were found in the right occipital fusiform gyrus (OFG), whereas the right temporal-occipital fusiform cortex (TOFC) was found when the spherical model was used. This difference is even higher when analyzing the results for ADHD patients, since the right OFG is found when the realistic head model is used, whereas the left OFG is found when the spherical head model is considered. Note also that when analyzing SCDP for words stimuli, the left OFG was found in all cases. However, it has to be remarked that the SCDP value is higher when the realistic model is considered, and therefore results will be more accurate.

These differences between models may be explained in terms of the variance ratio introduced in Section 2.5. Figure 6 shows the variance ratio between the spherical and the realistic head models.

It can be seen that this measure is predominantly larger than unity, which means that the realistic head model is more reliable than the spherical model. Note that in the occipital pole (OP) and OFG the relation is up to 5 times, which means that the realistic head model will improve the spherical head model even better in these cortex areas, which are of special interest in the source localization of the N170 component.

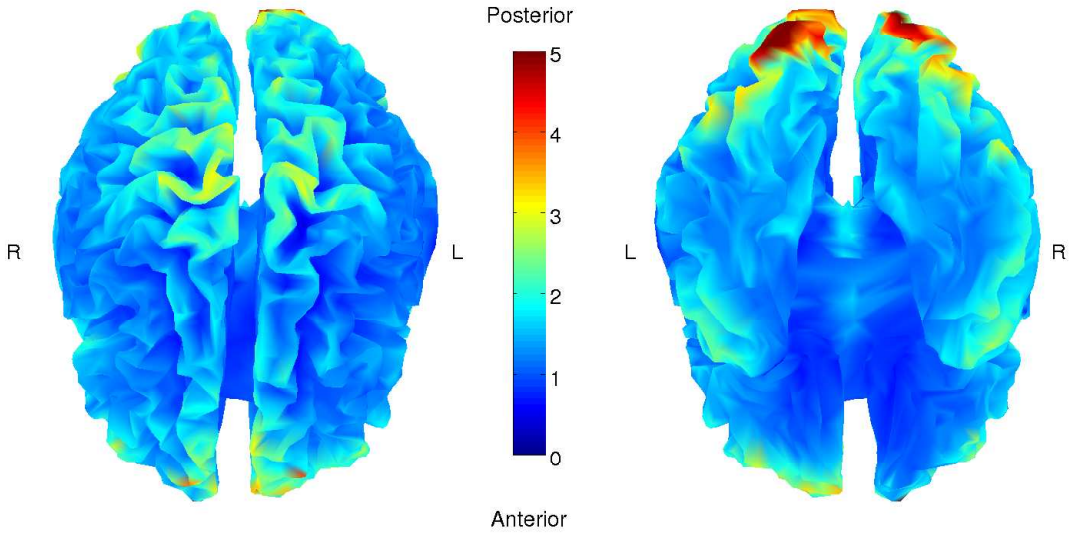

Figure 6. Superior (left) and basal (right) view of the brain showing the bias ratio (equation (1)). Larger values will be associated with cortex regions where the realistic model improves the source localization over the spherical model. Note that in the occipital pole and occipital fusiform gyrus the relation is up to 5 times.

4. Conclusions

In this work we show the influence of the head model considered in the forward problem for the ERP N170 component source localization. We show an accurate way to build an atlas based fully-realistic model, considering both geometry and electrical conductivity. Based on the sLORETA source imaging method we compare the influence of both models for source localization by means of the variance ratio on source reconstruction over the cortex. We find that the realistic head model improves the spherical head model, specially when the dipolar source model is considered. We also find that, using the proposed model, N170 sources are mainly located in the right OFG for both faces and simultaneous faces-word stimuli, and in the left OFG for words stimuli. Although these results are found to be the same for control subjects and ADHD patients, a notorious decrease of the SCPD value is found between them. This decrease in SCPD could be a possible marker of ADHD. In these situations, the realistic head model leads to more reliable results. Further work will be focused to analyze an accurate method to report activation areas considering distributed source localization results.

Acknowledgements

This work was funded by ANPCyT PICT 2007-00535, UNLP 11-I-0127, and ANPCyT PICT 2005-35423. The work of LB, AB, NvE, AP and AI was supported by CONICET. The work of CHM was also supported by CICpBA.

Group	Head Model	Faces			Faces + Words			Words		
		MNI Coordinates (x, y, z)	Hemisphere/ Anatomical Description	SCDP (10^{-6})	MNI Coordinates (x, y, z)	Hemisphere/ Anatomical Description	SCDP (10^{-6})	MNI Coordinates (x, y, z)	Hemisphere/ Anatomical Description	SCDP (10^{-6})
Control	Realistic	(40,-66,-15)	Right 45% OFG 15% LOC(id) 5% TOF	25.30	(26,-75,-15)	Right 74% OFG 7% LG	15.09	(-29,-80,-19)	Left 48% OFG 9% LOC(id)	9.44
	Spherical	(39,-57,-13)	Right 29% TOFC 8% OFG	6.85	(34,-58,-18)	Right 64% TOFC 16% OFG	3.90	(-22,-82,-20)	Left 26% OFG 5% LG	2.68
ADHD	Realistic	(25,-85,-17)	Right 49% OFG 9% LOC(id) 5% OP	12.27	(20,-85,-19)	Right 20% OFG 6% LOC(id)	9.00	(-24,-86,-20)	Left 35% OFG 8% LOC(id)	8.23
	Spherical	(-27,-72,-17)	Left 67% OFG	3.52	(-27,-72,-17)	Left 53% OFG	2.31	(-22,-82,-20)	Left 26% OFG 5% LG	2.35

Table 1. Anatomical locations of maximum estimated current density power (SCDP) for each group and stimuli condition (faces, words and simultaneous faces and words) using spherical and realistic head models. OFG: Occipital Fusiform Gyrus, LOC(id): Lateral Occipital Cortex (inferior division), TOFC: Temporal Occipital Fusiform Cortex, LG: Lingual Gyrus, OP: Occipital Pole. Cortex areas with probability less than 5% were not considered.

References

[1] von Ellenrieder N, Muravchik C and Nehorai A 2006 *IEEE Trans. Biomed. Eng.* **53** 249–257
[2] Güllmar D, Haueisen J and Reichenbach J 2010 *Neuroimage* **51** 145–163
[3] Beltrachini L, von Ellenrieder N and Muravchik C H 2010 *Comput Methods Programs Biomed.* In press
[4] de Munck J and Peters M 1993 *IEEE Trans. Biomed. Eng.* **40** 1166–1174
[5] von Ellenrieder N, Muravchik C, Wagner M and Nehorai A 2009 *IEEE Trans. Biomed. Eng.* **56** 587–597
[6] Valdés-Hernndez P, von Ellenrieder N, Ojeda-Gonzalez A, Kochen S, Alemán-Gómez Y, Muravchik C and Valdés-Sosa P 2009 *Journal of Neuroscience Methods* **185** 125–132
[7] Pascual-Marqui R 2002 *Methods & Findings in Experimental & Clinical Pharmacology* **24** 5–12
[8] Proverbio A, Riva F, Martin E and Zani A 2010 *PLoS.One* **5** e11242
[9] Rossion B, Joyce C, Cottrell G and Tarr M 2003 *Neuroimage* **20** 1609–1624
[10] Deffke I, Sander T, Heidenreich J, Sommer W, Curio G and Trahms L 2007 *Neuroimage* **35** 1495–1501
[11] Mnatsakanian E and Tarkka I 2004 *Clin. Neurophysiol.* **115** 880–886
[12] Schweinberger S, Pickering E, Jentzsch I, Burton A and Kaufmann J 2002 *Cognitive Brain Research* **14** 398–409
[13] Itier R and Taylor M 2004 *Neuroreport* **15** 1261–1265
[14] Marsh P and Williams L 2006 *Neuroscience and Biobehavioral Reviews* **30** 651–665
[15] Ibáñez A, Manes F, Escobar J, Trujillo N, Andreucci P and Hurtado E 2010 *Neuroscience Letters* **471** 48–52
[16] Ibáñez A, Petroni A, Urquina H, Torralva T, Blenkmann A, Beltrachini L, Muravchik C, Baez S, Cetckovih M, Torrente F, Hurtado E, Guex R, Sigman M, Lischinsky A and Manes F 2011 *Social Neuroscience* In press
[17] American Psychiatric Association 2000 *Diagnostic and statistical manual of mental disorders (4th ed., text rev.)* (Amer Psychiatric Pub)
[18] Gratton G, Coles M and Donchin E 1983 *Electroencephalography and Clinical Neurophysiology* **55** 468–484
[19] Dannhauer M, Lanfer B, Wolters C and Knösche T 2010 *Human Brain Mapping* In press
[20] Mazziotta J, Toga A, Evans A, Fox P, Lancaster J, Zilles K, Woods R, Paus T, Simpson G, Pike B, Holmes C, Collins L, Thompson P, MacDonald D, Iacoboni M, Schormann T, Amunts K, Palomero-Gallagher N, Geyer S, Parsons L, Narr K, Kabani N, Goualher G L, Boomsma D, Cannon T, Kawashima R and Mazoyer B 2001 *Philos. Trans. R. Soc. Lond. B Biol. Sci.* **356** 1293–1322
[21] Jenkinson M, Pechaud M and Smith S 2005 *Eleventh Annual Meeting of the Organization for Human Brain Mapping*
[22] Mori S, Oishi K, Jiang H, Jiang L, Li X, Akhter K, Hua K, Faria A, Mahmood A, Woods R, Toga A, Pike G, Neto P R, Evans A, Zhang J, Huang H, Miller M, van Zijl P and Mazziotta J 2008 *Neuroimage* **40** 570–582
[23] Tuch D, Wedeen V, Dale A, George J and Belliveau J 2001 *Proc. Natl. Acad. Sci. USA* **98** 11697–11701
[24] Beltrachini L, von Ellenrieder N and Muravchik C H 2008 *Actas del XVII Congreso sobre Métodos Numéricos y sus Aplicaciones - ENIEF*
[25] Fang Q and Boas D 2009 *Proceedings of IEEE International Symposium on Biomedical Imaging* 1142–1145
[26] Sekihara K, Sahani M and Nagarajan S 2005 *Neuroimage* **25** 1056–1067
[27] Greenblatt R, Ossadtchi A and Pflieger M 2005 *IEEE Trans. Signal Process.* **53** 3403–3412
[28] Desikan R, Segonne F, Fischl B, Quinn B, Dickerson B, Blacker D, Buckner R, Dale A, Maguire R, Hyman B, Albert M and Killiany R 2006 *Neuroimage* **31** 968–980